J Therm Anal Calorim (2014) 117:93–99
DOI 10.1007/s10973-014-3639-0

Thermodynamic study of the eutectic Mg_{49}–Zn_{51} alloy used for thermal energy storage

J. Rodríguez-Aseguinolaza · P. Blanco-Rodríguez · E. Risueño · M. J. Tello · S. Doppiu

Received: 29 August 2013 / Accepted: 4 January 2014 / Published online: 31 January 2014

Abstract The eutectic Mg_{49}–Zn_{51} (mass%) alloy has been identified as a suitable material for latent heat thermal energy storage. Within this scope, the exhibited solid–solid and solid–liquid phase transitions have been carefully characterized. A detailed thermodynamic study focused on the specific heat of the investigated alloy is also provided. The C_p behaviour, very important in the thermal energy storage frame, is theoretically modelled and experimentally validated by quasi-isothermal modulated differential scanning calorimetry measurements. Different intermetallic phases of the Mg–Zn binary system have also been successfully described within this approach in the complete temperature range.

Keywords Differential scanning calorimetry (DSC) · Specific heat · Phase transformations · Thermal energy storage · Mg–Zn binary alloys · Thermodynamics

Introduction

Thermal energy storage [1–3] has been revealed as a key factor in the efficient use of the energy sources and the different heat production processes [4–6]. Several sensible and latent heat-based storage methods have been widely explored in the last years [1, 2, 7, 8]. The second one, which presents important advantages, consists on the supply and recovery of the latent heat (ΔH) of a first-order phase transition (usually solid–liquid) of a suitable material, which occurs at a constant temperature.

A wide variety of materials with potential use in the latent heat storage frame have been considered according to their latent heat or transformation temperature [3, 9–13]. Salt solutions have been studied for the low-temperature range (243–273 K) with a transformation enthalpy between 230 and 330 J g^{-1} [12], and paraffins, fatty acids or salt hydrates for the middle-temperature range (273–373 K) with enthalpy values between 130 and 260 J g^{-1} [12, 14–16]. At higher temperatures a few available phase change materials (PCM) are found [17]. The main shortcoming of most of these compounds is their low thermal conductivity, between 0.4 and 5 W m^{-1} K^{-1} [10, 12, 18, 19], which limits considerably the heat transfer in the material.

In order to overcome this drawback, metallic materials have been proposed as latent heat storage materials [10, 20–22]. Previous works have shown the capabilities of metallic pure elements (Al, Zn, Na, Cu, Mg or Ca) or alloys (Al–Mg, Al–Si, Al–Cu–Mg, Mg–Si, …), whose melting temperatures are found between 613 and 1,218 K and transformation enthalpies are between 140 and 775 J g^{-1} approximately [23, 24]. In this work, the Mg–Zn binary system has been identified to be of particular interest as it presents an eutectic composition, Mg_{49}–Zn_{51} (mass%), which matches the requirements concerning melting–solidification temperature and storage energy density [23] for direct steam generation in a concentrated solar power plant.

The aim of this work, which is part of a systematic investigation of Mg–Zn and Mg–Zn–Al alloys in our laboratories, is to provide a complete thermodynamic analysis

J. Rodríguez-Aseguinolaza (✉) · P. Blanco-Rodríguez · E. Risueño · S. Doppiu
CIC Energigune, Albert Einstein 48, 01510 Miñano, Álava, Spain
e-mail: jrodriguez@cicenergigune.com

M. J. Tello
Depto. Física de la materia condensada, Facultad de ciencia y tecnología, Universidad del País Vasco, Apdo. 644, 48080 Bilbao, Bizkaia, Spain

of the eutectic Mg_{49}–Zn_{51} alloy as PCM for thermal energy storage.

Experimental

Eutectic Mg_{49}–Zn_{51} alloy synthesis

The alloy was synthesized by mixing both metals in the proportions associated to the eutectic composition, 49 % of Mg and 51 % Zn (mass%) according to the Mg–Zn phase diagram [25] and confirmed by later assessments [26, 27]. Zn and Mg were obtained from 99.995 to 99.94 % purity ingots, respectively. The pieces were placed in an alumina crucible inside a stainless steel container hermetically closed under argon atmosphere using a copper sealing plate. The container was heated up to 923 K and was isothermally maintained for 12 h ensuring an appropriate diffusion time. A rotatory movement was also applied to favour the homogeneity of the alloy. After cooling down to room temperature at slow rate (around 0.1 K min^{-1}), a solid ingot of eutectic Mg_{49}–Zn_{51} alloy was obtained. X-ray experiments confirmed that there was no diffusion between the alloy and the crucible. This procedure guarantees the presence of the expected equilibrium phases at room temperature, according to the mentioned phase diagram of the alloy and avoids the formation of metastable phases. In addition, no mass loss has been observed during the alloy synthesis process. The correct composition of the synthesized samples has been confirmed by calorimetric measurements which show the peaks associated to the transformation events according to the phase diagram of the alloy.

Calorimetric measurements

The phase transitions present in the synthesized eutectic Mg_{49}–Zn_{51} alloy have been investigated between 473 and 723 K at different heating/cooling rates using a thermal analysis (TA) Q2000 differential scanning calorimeter. The experimental error for the temperature and the enthalpy are around ±0.01 K and ±0.1 % in each case. Alumina sample holders were used in the melting/solidification experiments, avoiding corrosion phenomena in the liquid phase. All the runs were carried out under argon inert atmosphere preventing the alloy from oxidation.

The specific heat of the eutectic Mg_{49}–Zn_{51} alloy has been measured using the modulated quasi-isothermal DSC technique, described in references [28, 29]. In our experiments the modulation time, amplitude and period have been fixed to 1 h, 1 K and 120 s, respectively. The sample has been polished to ensure a good contact with the highly conductive aluminium pan. The thickness of the sample was around 1.5 mm to avoid temperature gradients. The mass of the Mg_{49}–Zn_{51} alloy was 23.829 mg, which provided a good calorimetric signal. Using this procedure, in this work, the specific heat is measured every 4 K from 193 to 473 K with an experimental error lower than ±3 %. X-ray diffraction experiments confirm that there is no diffusion between the eutectic Mg_{49}–Zn_{51} alloy and the aluminium pans in the measured temperature range (solid phase). Moreover, after the measurements, no mass change or oxidation has been found in the alloy.

Experimental results

Various standard DSC experiments at different heating/cooling rates have been performed. At 5 and 10 K min^{-1} rates two partially overlapped transformation peaks have been found on heating and cooling. At 1 K min^{-1} rate, Fig. 1 shows two clear separate transformation peaks on the heating run, which permits to analyse each transformation event separately. According to the Mg–Zn phase diagram [25, 26], the first peak, with $T_1^h = 608.3$ K onset temperature and $\Delta H_1^h = 24.8$ J g^{-1} enthalpy, corresponds to the eutectoid reaction of the MgZn intermetallic phase (also identified as $Mg_{12}Zn_{13}$ [30] and $Mg_{21}Zn_{25}$ with trigonal structure, space group $R\bar{3}c$ [31]) and Mg. This leads to the formation of the $Mg_{51.04}Zn_{19.80}$ (orthorhombic structure, space group Immm [32]) intermetallic compound. The second peak at $T_2^h = 614.5$ K corresponds to the melting process of the eutectic alloy with a latent heat of $\Delta H_2^h = 130.2$ J g^{-1}. Overall, the total enthalpy value of both transformation processes is $\Delta H_T^h = 155.0$ J g^{-1}, in agreement with [23].

On cooling, both peaks are partially overlapped, even at 0.5 K min^{-1} cooling rate. The onset temperature of the solidification process is found at $T_2^c = 606.6$ K while the eutectoid reaction onset temperature cannot be accurately determined. However, $T_1^c = 605.4$ K approximated value is obtained by extrapolation of the DSC peak. Based on the onset temperatures of the melting–solidification process and the eutectoid reaction the thermal hysteresis values are $\Delta T_2 = 7.9$ K and $\Delta T_1 = 2.9$ K, respectively. The determination of the individual transformation enthalpies is difficult in this case, but the total value of both processes is $\Delta H_T^c = 153.0$ J g^{-1}.

When heating at 5 and 10 K min^{-1}, the obtained eutectoid reaction temperatures are $T_1^h = 605.6$ K and $T_1^h = 606.5$ K, respectively. The melting temperatures are similar to the value found at 1 K min^{-1}. On cooling, the measured solidification temperatures are $T_2^c = 604.3$ K at 5 K min^{-1} and $T_2^c = 603.6$ K at 10 K min^{-1}. In the three investigated rates no changes on the total enthalpy value have been found.

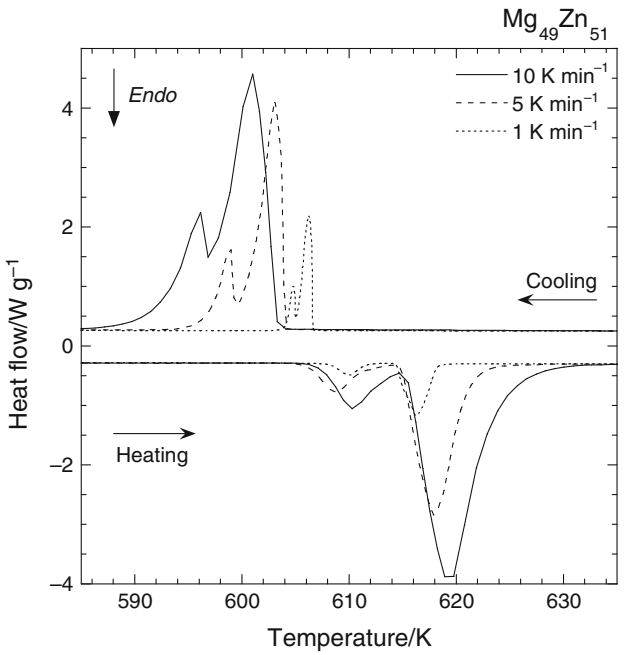

Fig. 1 DSC results for the eutectic Mg_{49}–Zn_{51} alloy at 10, 5 and 1 K min^{-1} heating/cooling rates. Exception made for the 1 K min^{-1} heating run, two overlapped transformations peaks have been found in the performed DSC experiments

The differences on the solidification process, shown in Fig. 1, which are dependent on the cooling rate, might influence the nucleation process of the alloy. In addition, due to the different thermal hysteresis values, both transformation processes are closer in temperature on the cooling run. As no thermal equilibrium is attained during the measurement, the eutectoid reaction could start before the solidification process is completed. Overall, these phenomena might influence the nucleation process of the solid phases and the subsequent eutectoid reaction on consecutive thermal cycles. As a consequence, different eutectoid reaction behaviours and temperatures can be expected. This may explain the discrepancy on the eutectoid reaction temperatures between the value obtained in this work and the ones given by [26] and [27], $T_1^h = 598.2$ K and $T_1^h = 594$ K, respectively. The small difference of the total enthalpy value measured on heating and cooling, around 1 %, which is larger than the experimental error, might also be related to similar mechanisms. Anyway, further investigation is needed to clarify this behaviour.

Theoretical lattice specific heat calculation of the Mg_{49}–Zn_{51} alloy

The thermodynamic functions, such as the enthalpy, entropy or Gibbs energy, determine the thermal behaviour of a material. For this reason, when a sensible or latent heat storage device is designed, $H(T), S(T)$ and $G(T)$ are usually required. All these functions can be numerically obtained from the specific heat data. As a consequence, the knowledge of the specific heat of the storage material becomes of great importance. The lattice specific heat of a compound can be determined in the complete temperature range using a theoretical model based on the addition of the harmonic, electronic and anharmonic contributions. However, due to the lack of complete experimental data about the investigated alloy, the specific heat has to be calculated within an approximated frame.

Harmonic contribution

The harmonic lattice specific heat (C_h), which in general can be assumed to be the specific heat at constant volume (C_v) can be directly obtained from the Debye model using Eq. (1). For both metals, Mg and Zn, this model assumes a parabolic distribution of the phonon density of states (DOS) given by Eq. (2) where v_D is the Debye's cut-off frequency:

$$C_h = C_v = 3nk_B\left(\frac{T}{\theta_D}\right)^3 \int_0^{\theta_D/T} \frac{x^4 e^x}{(e^x-1)^2}dx \tag{1}$$

$$g(v) \propto v^2 \, (0 \le v \le v_D) \tag{2}$$

In Eq. (1), n is the number of atoms per unit mass, θ_D is the empirical Debye temperature, k_B is the Boltzmann constant and h is the Planck constant. The Debye's cut-off frequency (v_D) and the variable (x) of Eq. (1) are given by Eqs. (3) and (4), respectively.

$$v_D = \frac{k_B\theta_D}{h} \tag{3}$$

$$x = \frac{hv_D}{k_BT} \tag{4}$$

In order to obtain accurate numerical results, the Debye integral (Eq. 1) has been expanded by means of a polynomial fitting as a function of the coefficient $\left(\frac{\theta_D}{T}\right)$ in two separate temperature ranges, as shown in Eq. (5). Conventionally, the high and low temperature limit between both ranges has been established in $T = \left(\frac{\theta_D}{25}\right)$.

$$C_h = C_v = \begin{cases} \sum_{n=0}^{20} a_n\left(\frac{\theta_D}{T}\right)^n & \text{if} \quad T \ge \left(\frac{\theta_D}{25}\right) \\ \frac{b}{\left(\frac{\theta_D}{T}\right)^3} & \text{if} \quad T < \left(\frac{\theta_D}{25}\right) \end{cases} \tag{5}$$

Using this procedure the harmonic specific heat of each individual metallic component of the alloy, Mg and Zn, has been calculated. In the literature different characteristic Debye temperatures (θ_D) of both metals can be found [33–36]. However, the best results are obtained selecting

$\theta_D^{Mg} = 318$ K and $\theta_D^{Zn} = 234$ K [34]. The harmonic lattice specific heats averaged by the mass percentage of each component of the alloy, 49 % Mg and 51 % Zn, respectively, are shown in Fig. 2 (C_h^{Mg} and C_h^{Zn}). The addition of both contributions as shown in Eq. (6) gives the total harmonic specific heat of the Mg_{49}–Zn_{51} eutectic alloy (curve 1 in Fig. 2).

$$C_h^{alloy} = C_v^{alloy} = 0.49C_h^{Mg} + 0.51C_h^{Zn} \quad (6)$$

Electronic contribution

Within the free electron model, which is valid to describe most of the metallic elements, this contribution to the total lattice specific heat is given by Eq. (7). Except at low temperatures, it is usually very small when compared with the harmonic contribution of the lattice. Its value at room temperature represents around a 0.5 % of the total specific heat.

$$C_e = \frac{\pi^2 k_B^2 n}{2\varepsilon_F} T \quad (7)$$

In Eq. (7) k_B is the Boltzmann constant, n is the number of electrons in the conduction band and ε_F is the Fermi energy.

In the Mg_{49}–Zn_{51} eutectic alloy each metal contributes with two electrons to the conduction band. As a consequence, the electron number per unit mass in the conduction band is given by Eq. (8) as a function of the Avogadro's number ($N_A = 6.022 \times 10^{23}$) and the atomic mass of each element (A).

$$n = \frac{2N_A}{A} \quad (8)$$

Taking into account that Fermi's energy values are $\varepsilon_F = 7{,}08$ eV for Mg and $\varepsilon_F = 9{,}47$ eV for Zn [37], the electronic contribution to the specific heat of the eutectic alloy as a function of temperature is given by Eq. (9) in terms of the averaged individual contribution (mass%).

$$\begin{aligned} C_e^{alloy} &= 0.49C_e^{Mg} + 0.51C_e^{Zn} \\ &= 0.49 \cdot 4.11 \times 10^{-5} T + 0.51 \cdot 1.14 \times 10^{-5} T \end{aligned} \quad (9)$$

At room temperature ($T = 298.15$ K), the electronic contribution is $C_e^{alloy} = 0.0077$ J g^{-1}K^{-1}, which represents around 1 % of the harmonic lattice contribution to C_p. This is a noticeably high value compared with other metallic elements or alloys. However, this behaviour might be explained by the electronic band structure of the transition metals like Zn which usually leads to high electronic specific heat [33]. The addition of the harmonic and electronic contributions, $C_h^{alloy} + C_e^{alloy}$, leads to the curve 2 of Fig. 2. As can be seen, both contributions clearly underestimate the experimental value of the C_p baseline of the eutectic alloy (circled line in Fig. 2). This difference can be associated to the anharmonic contribution to the total lattice C_p.

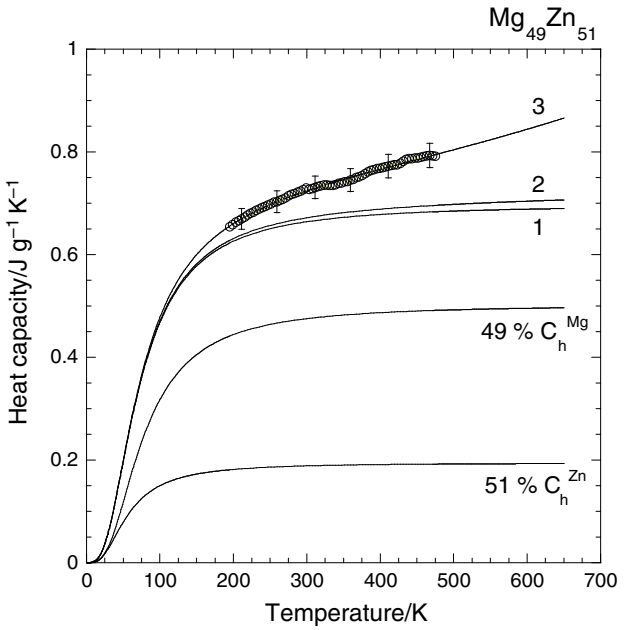

Fig. 2 *Circles* represent the experimental C_p value of the eutectic Mg_{49}–Zn_{51} alloy obtained by modulated differential scanning calorimetry. *Curve 1* harmonic specific heat of the alloy (C_h^{alloy}); *2* harmonic+electronic specific heat ($C_h^{alloy} + C_{elec}^{alloy}$); *3* harmonic+electronic+Nernst–Lindemann anharmonic specific heat ($C_h^{alloy} + C_{elec}^{alloy} + C_{anh}^{alloy}$)

Anharmonic contribution

For isotropic materials, it can be shown that the anharmonic contribution is given by Eq. (10).

$$C_{anh} = C_p - C_v = TV\frac{\alpha^2}{k_T} \quad (10)$$

where T is the absolute temperature, V is the specific volume, α is the volume thermal expansion coefficient and k_T is the isothermal compressibility.

For anisotropic materials this relation can be generalized as a function of the elastic constant tensor (c_{ijkl}), as shown in Eq. (11).

$$C_{anh} = C_p - C_v = TV \sum_{i,j,k,l=1}^{3} c_{ijkl}\alpha_{ij}\alpha_{kl} \quad (11)$$

Taking into account the symmetry of the crystal, Eq. (11) can be simplified. However, this procedure implies the knowledge of the elastic constant tensor which is not available for the eutectic Mg_{49}–Zn_{51} alloy. As a consequence, in order to obtain the anharmonic contribution to the lattice specific heat, a phenomenological model is necessary. One alternative is the Nernst–Lindemann semiempirical relation, shown in Eq. (12). It is based on

Grüneisen equation and it states that the anharmonic contribution is proportional to the product of the absolute temperature and the squared total lattice specific heat (C_p).

$$C_{anh} = C_p - C_v = aTC_p^2 \quad (12)$$

In Eq. (12), a is an empirical parameter, given by Eq. (13), which depends on the material. It has a nearly constant value over a wide range of temperature.

$$a = \frac{V\alpha^2}{C_p^2 k_T} \quad (13)$$

If any of the expansivity parameters is not known, one alternative is to empirically fit the measured C_p baseline by changing the value of the a constant. Using the harmonic specific heat values of the alloy obtained from Eq. (6), the anharmonic contribution can be calculated in the complete temperature range by solving Eq. (12) for C_p and selecting empirically $a = 3.4 \times 10^{-4}$ g J^{-1}. It can be noted that the value of this constant is similar to the one found for pure Zn and it is close to the value corresponding to Cu (3×10^{-4} g J^{-1}).

Finally, curve 3 of Fig. 2 shows the theoretical specific heat of the eutectic Mg_{49}–Zn_{51} alloy $\left(C_h^{alloy} + C_e^{alloy} + C_{anh}^{alloy}\right)$ together with the experimental C_p values obtained by modulated DSC (circles in Fig. 2). It can be noted that the difference between theoretical and experimental values is lower than 3 %.

For comparison, as an example, the experimentally obtained C_p value of the eutectic Mg_{49}–Zn_{51} alloy at room temperature is $C_p^{alloy}(298.15) = 0.73$ J g^{-1} K^{-1}. Calculating the weighted average specific heat at the same temperature from the experimental values of the individual metallic elements ($C_p^{Mg}(298.15) = 1.024$ J $g^{-1}K^{-1}$ and $C_p^{Zn}(298.15) = 0.388$ J $g^{-1}K^{-1}$ [37]), the obtained result is $C_p^{average} = 0.70$ J $g^{-1}K^{-1}$. Finally, the C_p value predicted by the thermodynamic model explained above is $C_p^{alloy} = 0.72$ J $g^{-1}K^{-1}$. In all the three cases the data dispersion is contained within a ±4 %.

This theoretical model provides an accurate specific heat baseline in the complete temperature range. Its direct numerical integration allows the calculation of the thermodynamic functions of the eutectic alloy. Within this frame, the transformation thermodynamic functions can also be obtained. The thermodynamic equilibrium temperature of the eutectoid reaction and melting/solidification process can be defined as the average temperature between the heating and cooling transformation events: $T_{eq1} = 606.85$ K and $T_{eq2} = 610.55$ K, respectively. Equation (14) gives the entropy change in both cases.

$$\Delta S = \frac{\Delta H}{T_{eq}} \quad (14)$$

The obtained values are $\Delta S_1(T_{eq1}) = 0.04$ J g^{-1} K^{-1} and $\Delta S_2(T_{eq2}) = 0.21$ J g^{-1} K^{-1}, respectively. Finally, the driving force of the melting and solidification process of the alloy can be calculated from Eq. (15).

$$\Delta G(T) = \left|G_{liquid}(T) - G_{solid}(T)\right| \quad (15)$$

The respective values are $\Delta G_m(T_2^h = 614.5\ K) \approx \Delta G_s(T_2^c = 606.6\ K) \approx 0.84$ J g^{-1}.

Application to other Mg–Zn alloys

This thermodynamic model has also been applied to several Mg–Zn intermetallic compounds. Morishita et al. [38] have reported the specific heat values of the $Mg_{25.55}$–$Zn_{74.45}$, $Mg_{19.86}$–$Zn_{80.14}$, $Mg_{15.66}$–$Zn_{84.34}$ and $Mg_{6.34}$–$Zn_{93.66}$ (mass%) alloys in the 2–700 K temperature range. As indicated in [38], C_p was measured using the so-called 'relaxation technique' for the 2–400 K range and by DSC for the 400–700 K range.

For each alloy, the harmonic and electronic contributions to the total specific heat are directly obtained selecting the individual metal compositions (mass%) on each case. On the other hand, the anharmonic contribution depends on the material. The thermophysical properties

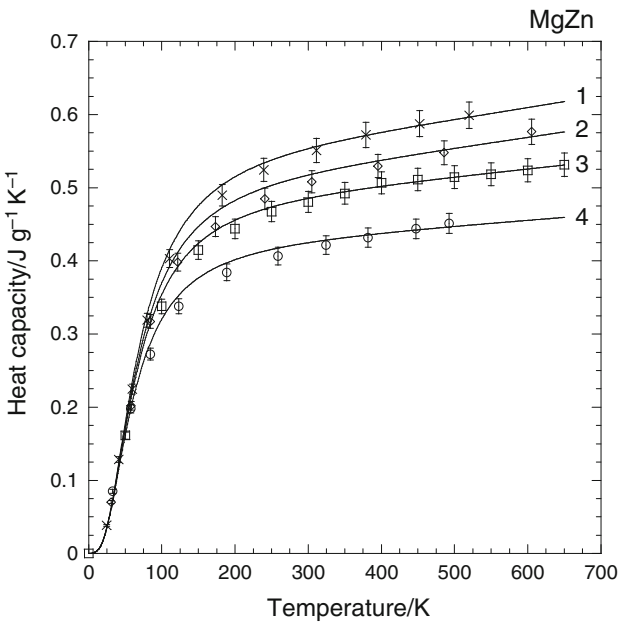

Fig. 3 Model predicted (*continuous lines*) and experimental specific heat data (*points*) of the different Mg–Zn alloys. Respectively *1* and *times* $Mg_{25.55}$-$Zn_{74.45}$; *2* and *open diamond* $Mg_{19.86}$–$Zn_{80.14}$; *3* and *open square* $Mg_{15.66}$–$Zn_{84.34}$; *4* and *open circle* $Mg_{6.34}$–$Zn_{93.66}$

that determine the anharmonic contribution associated to different intermetallic compounds might show noticeable changes leading to different C_{anh} values. In this model, this contribution is empirically determined selecting the a constant in Eq. (12) for each different alloys. The selected values have been $a = 2.7 \times 10^{-4}, 2.9 \times 10^{-4}, 2.4 \times 10^{-4}$ and 2.4×10^{-4} g J^{-1} for $Mg_{25.55}$–$Zn_{74.45}$, $Mg_{19.86}$–$Zn_{80.14}$, $Mg_{15.66}$–$Zn_{84.34}$ and $Mg_{6.34}$–$Zn_{93.66}$, respectively. The comparison between the reported experimental C_p data and that predicted by the model is shown in Fig. 3, where a very good agreement is found at low temperatures in all cases. However, the model overestimates the experimental data around 3 % in the medium temperature range (100–250 K). This behaviour might be due to the simplicity of the phonon spectrum assumed by the Debye model, used to determine the harmonic contribution. The high-temperature range, where the anharmonic contribution is more relevant, is also successfully described.

Conclusions

To conclude, the phase transformation behaviour of the Mg_{49}–Zn_{51} eutectic alloy proposed as PCM for thermal energy storage has been studied. A simple thermodynamic model has been developed to calculate the lattice specific heat of the eutectic Mg_{49}–Zn_{51} (mass%) alloy and different intermetallic phases of the Mg–Zn binary system in the complete temperature range. In all cases, a very good agreement has been found between the theoretical calculation and the experimental C_p data. However, the knowledge of the phonon spectra or the elastic constants could lead to even more accurate results in the low-intermediate temperature range. This model also allows calculating the thermodynamic functions of the alloy. Finally, within the thermal energy storage frame where C_p plays a capital role, this theoretical calculation is a powerful predictive tool which can be generalized for other metallic alloys used as storage materials.

Acknowledgements The authors would like to acknowledge the support of the Department of Industry, Innovation, Commerce and Tourism of the Basque Government for funding the ETORTEK CIC Energigune-2011 research programme and also the University of the Basque Country (UPV/EHU).

References

1. Backmann G. Thermal energy storage: basics, design, applications to power generation and heat supply (topics in energy). New York: Springer; 1984.
2. Dinçer I, Rosen MA. Thermal energy storage: systems and applications. New York: Wiley; 2002.
3. Sharma A, Tyagi VV, Chen CR, Buddhi D. Review on thermal energy storage with phase change materials and applications. Renew Sustain Energy Rev. 2009;13:318–45.
4. Garg HP. Advances in solar energy technology, vol. 1. Dordrecht: D. Reidel/Kluwer; 2010.
5. Farid MM, Khudhair AM, Razack SAK, Al-Hallaj S. A review on phase change energy storage: materials and applications. Energy Convers Manag. 2004;45:1597–615.
6. Huggins RA. Energy storage. New York: Springer; 2010.
7. Gil A, Medrano M, Martorell I, Lázaro A, Dolado P, Zalba B, Cabeza LF. State of the art on high temperature thermal energy storage for power generation. Part 1: concepts, materials and modellization. Renew Sustain Energy Rev. 2010;14:31–55.
8. Medrano M, Gil A, Martorell I, Potau X, Cabeza LF. State of the art on high temperature thermal energy storage for power generation. Part 2: case studies. Renew Sustain Energy Rev. 2010;14:56–72.
9. Agyenim F, Hewitt N, Eames P, Smyth M. A review of materials, heat transfer and phase change problem formulation for latent heat thermal energy storage systems (LHTESS). Renew Sustain Energy Rev. 2010;14:615–28.
10. Kenisarin MM. High-temperature phase change materials for thermal energy storage. Renew Sustain Energy Rev. 2010;14:955–70.
11. Nomura T, Okinaka N, Akiyama T. Technology of latent heat storage for high temperature application: a review. ISIJ Int. 2010;9:1229–39.
12. Zalba B, Marín JM, Cabeza LF, Mehling H. Review on thermal energy storage with phase change: materials, heat transfer analysis and applications. Appl Therm Eng. 2003;23:251–83.
13. Parameshwaran R, Jayavel R, Kalaiselvam S. Study on thermal properties of organic ester phase-change material embedded with silver nanoparticles. J Therm Anal Calorim. 2013;114:845–58.
14. Meng X, Zhang H, Sun L, Xu F, Jiao Q, Zhao Z, Zhang J, Zhou H, Sawada Y, Liu Y. Preparation and thermal properties of fatty acids/CNTs composite as shape-stabilized phase change materials. J Therm Anal Calorim. 2013;111:377–84.
15. Tyagi VV, Pandey AK, Kaushik SC, Tyagi SK. Thermal performance evaluation of a solar air heater with and without thermal energy storage. J Therm Anal Calorim. 2012;107:1345–52.
16. Harikrishnan S, Deepak K, Kalaiselvam S. Thermal energy storage behavior of composite using hybrid nanomaterials as PCM for solar heating systems. J Therm Anal Calorim. 2013. doi:10.1007/s10973-013-3472-x.
17. Ren N, Wu Y, Wang T, Ma C. Experimental study on optimized composition of mixed carbonate for phase change thermal storage in solar thermal power plant. J Therm Anal Calorim. 2011;104:1201–8.
18. Wang N, Zhang XR, Zhu DS, Gao JW. The investigation of thermal conductivity and energy storage properties of graphite/paraffin composites. J Therm Anal Calorim. 2012;107:949–54.
19. Zeng JL, Cao Z, Yang DW, Xu F, Sun LX, Zhang XF, Zhang L. Effects of MWNTS on phase change enthalpy and thermal conductivity of a solid–liquid organic pcm. J Therm Anal Calorim. 2009;95(2):507–12.
20. Horsthemke A, Marschall E. NASA technical translation: storage in molten salts and metals, NASA-TT-F-17412; 1977.
21. Birchenall CE. NASA reports: heat storage in alloy transformations, NASA CR-159787; 1980.
22. Gasanaliev AM, Gamataeva BY. Heat-accumulating properties of melts. Russ Chem Rev. 2000;69(2):179–86.
23. Birchenall CE, Riechman AF. Heat storage in eutectic alloys. Metall Trans A. 1980;11A:1415–20.
24. Farkas D, Birchenall CE. New eutectic alloys and their heats of transformation. Metall Trans A. 1985;16A:323–8.
25. Clark JB, Zabdyr L, Moser Z. In: Massalki TB, editor. Binary alloy phase diagram. Materials Park: ASM; 1990. p. 2571.
26. Agarwal R, Fries SG, Lukas HL, Petzow G, Sommer F, Chart TG, Effenberg G. Z Met Kd. 1992;83(4):216–23.

27. Ghosh P, Mezbahul-Islam M, Medraj M. Critical assessment and thermodynamic modeling of Mg–Zn, Mg–Sn, Sn–Zn and Mg–Sn–Zn systems. CALPHAD. 2012;36:28–43.
28. Danley RL. New modulated DSC measurement technique. Thermochim Acta. 2003;402:91–8.
29. Reading M, Elliott D, Hill V. Proceedings of the 21st North American Thermal Analytical Society 1992; 145–50.
30. Clark JB, Rhines FN. Central region of the magnesium–zinc phase diagram. J Met. 1957;9:425–30.
31. Cerny R, Renaudin G. The intermetallic compound Mg_{21}–Zn_{25}. Acta Crystallogr C. 2002;58:54–5.
32. Higashi I, Shiotani N, Uda M, Mizoguchi T, Katoh H. The crystal structure of Mg_{51}–Zn_{20}. J Solid State Chem. 1981;36:225–33.
33. Gopal ESR. Specific heats at low temperatures. London: Heywood Books/Plenum Press; 1966.
34. Ashcroft NW, Mermin ND. Solid state physics. Fort Worth: Harcourt Brace College Publishers; 1976.
35. Kittel C, Kroemer H. Thermal physics. In: Freeman WH, editor; 1980.
36. Barron THK, White GK. Heat capacity and thermal expansion at low temperatures. New York: Kluwer/Plenum Press; 1999.
37. Lide DR editor. CRC handbook of chemistry and physics, 86th ed. Boca Raton: Taylor & Francis; 2006.
38. Morishita M, Yamamoto H, Shikada S, Kusumoto M, Matsumoto Y. Thermodynamics of the formation of magnesium–zinc intermetallic compounds in the temperature range from absolute zero to high temperature. Acta Mater. 2006;54:3151–9.